auxiliary antenna placed at the bottom of the handset terminal. Depending on a mobile system, this additional antenna enables exploitation of MIMO or the spatial-diversity technique in order to improve radio link quality. The proposed antenna placement in the terminal structure is shown in Figure 8.

REFERENCES

1. K.L. Wong, Planar antennas for wireless communication, Wiley–Interscience, Hoboken, NJ, 2003.
2. L.J. Chu, Physical limitations on omnidirectional antennas, J Appl Phys 19 (1948), 1163–1175.
3. J.S. McLean, A re-examination of the fundamental limits on the radiation Q of electrically small antennas, IEEE Trans AP 44 (1996), 672–676.
4. K. Skonieczny, A miniature antenna for handset terminal of 2G 3G cellular mobile systems, Masters thesis, Institute of Telecommunications and Acoustics, Wroclaw University of Technology, 2004 (in Polish).

A NEW BI-FACED LOG PERIODIC PRINTED ANTENNA

E. Ávila-Navarro,[1] J. M. Blanes,[1] J. A. Carrasco,[1] C. Reig,[2] and E. A. Navarro[3]

[1] Electronic Technology Division
Universidad Miguel Hernández
Av. Universidad s/n 03202 Elche, Spain
[2] Department of Electronic Engineering
Universitat de València
C. Dr Moliner 50
46100 Burjassot, Spain
[3] Department of Applied Physics and Electromagnetism
Universitat de València
C. Dr Moliner 50
46100 Burjassot, Spain

Received 10 August 2005

ABSTRACT: *In this paper, a new design of a broadband planar printed antenna based on the academic log periodic antenna is presented. The antenna consists of a series of printed dipoles, distributed on both faces of the substrate. Some configurations are explored, with a different number of printed dipoles. These are designed, simulated, fabricated, and measured. The calculated and measured return losses and radiation patterns are presented. The utility of the proposed antenna associated with its frequency bandwidth is better than 80%. The measured absolute gain is 6.5 dBi, and the front-to-back ratio is around 8 dB. The presented antenna should find wide applications in wireless communication systems and phased arrays.* © 2005 Wiley Periodicals, Inc. Microwave Opt Technol Lett 48: 402–405, 2006; Published online in Wiley InterScience (www.interscience.wiley.com). DOI 10.1002/mop.21363

Key words: *log periodic antenna; printed dipoles; multiband antennas*

1. INTRODUCTION

Printed antennas display, traditionally, a high quality factor (Q) and, consequently, a narrow wideband [1]. This intrinsic characteristics is a handicap for broadband applications (radar, wireless communications, and so forth) [2]. In recent years, a renovated effort is being carried out to develop new antenna geometries capable of offering improved bandwidth while keeping the inherent advantages of printed antennas, that is, low profile, low cost, easy fabrication, and direct integration with circuitry. In this sense, we should firstly mention the utilization of multilayer antennas, such as stacked patch antennas [3]. On the other hand, wideband matching schemes have been applied in the development of printed antenna arrays [4], particularly, the utilization of log periodic structures, with the development of patch antennas in the early approaches [5, 6] and slot antennas more recently [7, 8].

In this paper, we introduce a new log-periodic printed antenna configuration, consisting of several logarithmically scaled dipoles. The dipoles are placed alternatively on the upper and lower faces of the substrate. In this way, the dipoles are fed with the correct phase, thus avoiding the need for additional phase controllers for coplanar stripline (CPS) feeding [8]. The antenna is analyzed using a specifically developed code, based on the FDTD algorithm. Our code which has been tested extensively in very complex antennas [9], is now adapted for microstrip-planar structures. The return losses (S_{11}) are calculated at the feed line, thus providing excellent bandwidth in the 2–5-GHz band. The radiation pattern is calculated from the near-field components. In addition, the simulated FDTD results are tested against the measurements. The measurements are carried out using an E8363B network analyzer (Agilent Technologies), which is also used for the radiation-pattern measurements within the anechoic chamber.

2. DESIGN

The antenna design is based on the well-known log-periodic antenna-scaling principle. Following this basis, the antenna displays a periodic behaviour with the frequency logarithm [8]. The structure of the proposed antenna is shown in Figure 1. The printed dipoles are periodically scaled, with the longer element designed for the lower resonant frequency and the shorter one for the higher frequency. The antenna dimensions follow the periodicity relationship [10]:

$$\tau = \frac{l_m}{l_{m+1}} = \frac{s_m}{s_{m+1}} = \frac{w_m}{w_{m+1}}, \tag{1}$$

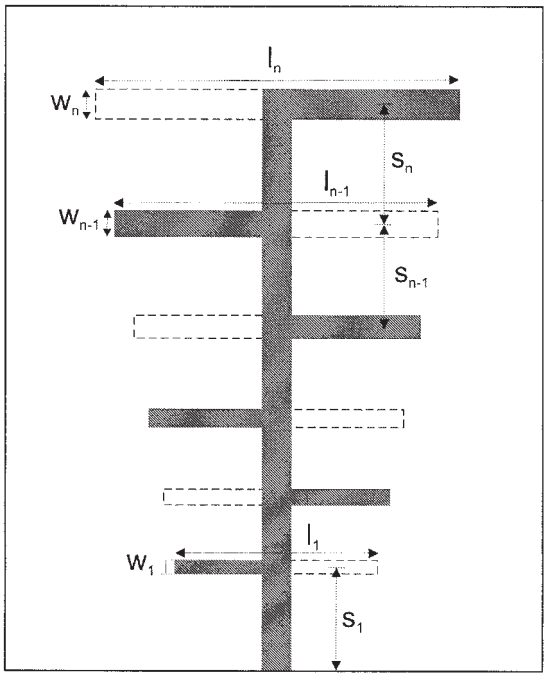

Figure 1 Antenna structure

TABLE 1 Design Parameters

4 Dipoles Configuration				
Dipole N°	Frequency [GHz]	*L* [mm]	*W* [mm]	*S* [mm]
1	2,93	38.84	2.04	31.8
2	2,58	44.14	2.32	18.92
3	2,27	50.16	2.64	21.5
4	2	57	3	24.43

8 Dipoles Configuration				
Dipole N°	Frequency [GHz]	*L* [mm]	*W* [mm]	*S* [mm]
1	4,89	23.29	1.22	18.88
2	4, 3	26.47	1.39	11.34
3	3,79	30.08	1.58	12.89
4	3,33	34.18	1.8	14.65
5	2,93	38.84	2.04	16.65
6	2,58	44.14	2.32	18.92
7	2,27	50.16	2.64	21.50
8	2	57	3	24.43

based on the dimensions defined in Figure 1. The feed is at the shortest dipole. In the following, we will refer to this antenna as the bi-faced log-periodic printed antenna (BiFaLPPA). The distance at which the first and shortest element is placed is critical for an optimal design. The best results for the antenna performance were obtained when this distance was, at least, a half-wavelength at the resonant frequency of the shortest dipole in the feed line. When a substrate with high dielectric constant is used, the dipole length is reduced. In our prototypes we used a clad substrate (ε_r = 3.2, thickness h = 1.52 mm), courtesy of Gil Technologies. For this specific substrate, the dipole length as a function of the resonant frequency is empirically given by

$$l_{dip} = 0.38\frac{c}{f}. \tag{2}$$

This relationship considerably reduces the overall size of the antenna by more than 20%, as compared with standard $\lambda/2$ printed-dipole-based antennas [11].

Following the proposed scheme, we designed several antennas with a different number of dipoles. A numerical general BiFaLPPA model was built using the FDTD technique, and the proposed designs were numerically analysed. Our FDTD model embeddes the 50Ω feed line where the incident and reflected voltages are sampled, including the connector transition between the feed line and the antennas' printed lines. Therefore, the model calculates the return losses associated with the actual mismatched coaxial line–printed line.

A Gaussian pulse was used as the time-domain excitation, with the appropriate frequency band. The electric-field components in the coaxial line were used to calculate the incident and reflected voltages, in order to obtain the return losses [9]. The Fourier transform of the electric-field tangential components in a closed surface containing the radiating parts, at some given frequencies, provided the near fields. From them, the radiation patterns were calculated.

3. RESULTS

The results for two specific models for two designed frequency bands, 2–3 GHz and 2–5 GHz, are presented. The two selected configurations have four and eight dipoles, respectively. In both cases, the parameter τ = 0.88 is used. The calculated design parameters are summarised in Table 1.

The FDTD results for the return losses for both configurations, as well as the measured results, are shown in Figure 2. From the figure, good agreement between calculations and measurements is easily observed, and the frequency bandwidth is straightforwardly derived as well. The four-dipole antenna has a frequency bandwidth of 2.55 GHz (82% of the central frequency), which is slightly wider than expected. We attribute this spreading to the contribution of the higher-order modes generated in the substrated and printed lines. In fact, the frequency of the next mode for the longer dipoles exactly agrees with the following peaks in the plot at 3.4 and 4.1 GHz. The eight-dipole antenna bandwidth was 1.77 GHz (65% of the central frequency). In this latter case, the frequency interval was narrower than expected. This difference may be related to the impedance mismatch of the shorter dipoles, at higher frequencies, partly associated with the higher-order modes. Even though these antennas were designed for 2–3 GHz and 2–5 GHz, for the proposed prototypes, good behaviour was obtained at the higher-frequency bands, which is a potentially useful feature for multiresonant applications.

Figure 3 shows the measured and calculated radiation patterns for both prototypes. For comparison, we selected the patterns at 2.0, 2.5, and 3.0 GHz. With regard to the return-loss results, good concordance was obtained between the measured and calculated results. The shape of the radiation patterns was found to be similar for all three frequencies. It can be observed that, as expected, the addition of shorter dipoles produces an enhancement in the directivity of the patterns, mainly in the E-plane.

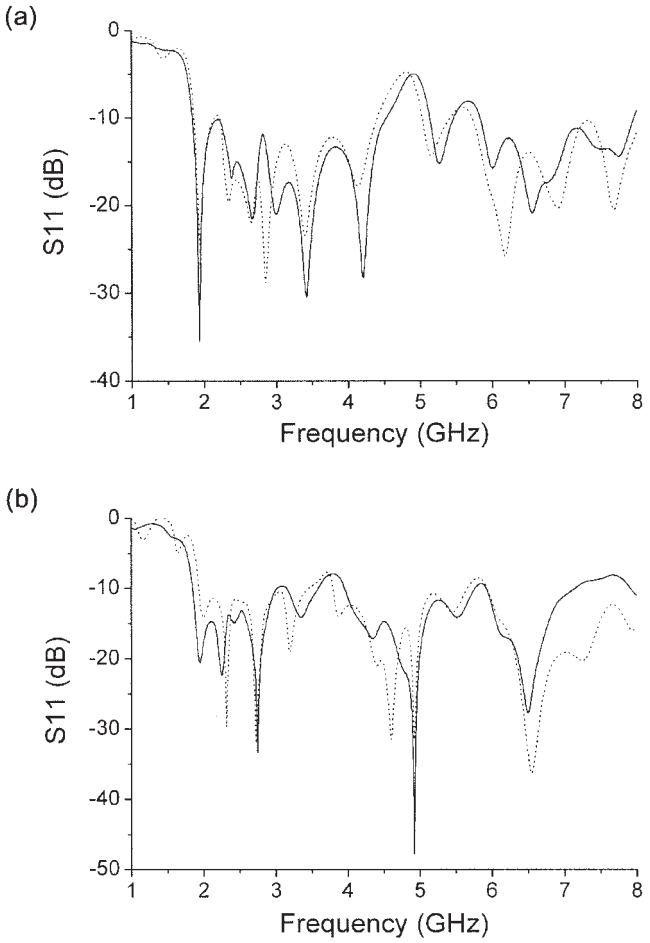

Figure 2 Return losses: (a) four-dipoles configuration; (b) eight-dipoles configuration (— measured, - - - simulated)

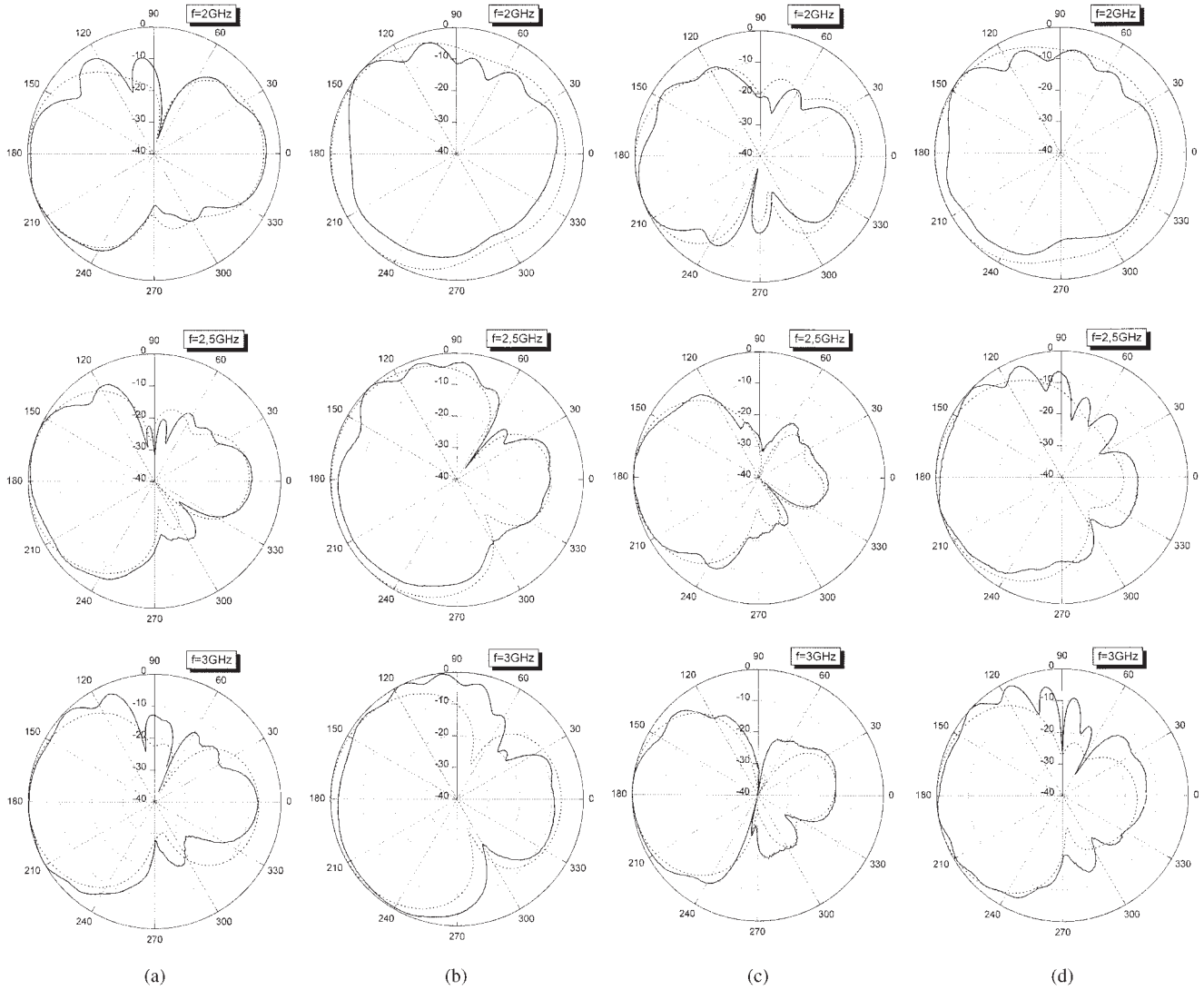

Figure 3 Four-dipoles configuration: (a) E-plane radiation pattern and (b) H-plane radiation pattern (— measured, - - - simulated); eight-dipoles configuration: (c) E-plane radiation pattern and (d) H-plane radiation pattern (— measured, - - - simulated)

Finally, we measured the gain of the antennas, obtaining a value close to 6.5 dBi for both configurations, which is slightly lower than the theoretical obtained values of 8.2 dBi. The front-to-back ratio is around 8 dB, and the E-plane and H-plane cuts exhibit broad single-beam patterns. The 1.7-dBi difference in the gain is due to the leaky-wave character of the antenna. It is possible to increase the gain by adding a large number of dipoles. In doing so, however, the dimensions of the antenna are also enlarged. The broad E-plane and H-plane beams of the radiation pattern and the large frequency band of these antennas are good features, demonstrating wide applications for phased arrays; therefore, the presented BiFaLPPA antennas should find wide applications as an array element.

4. CONCLUSION

We have successfully introduced a novel compact bi-faced log-periodic printed antenna (BiFaLPPA) with a large frequency bandwidth in the 2–3-GHz range, up to 80%. The directivity of the antenna is influenced by the number of dipole whereas the bandwidth and gain are less influenced by this parameter, which suggests a typical leaky-wave behavior. In addition, the FDTD technique has proved to be an effective tool for the analysis of these structures, thus providing excellent agreement between the numerical calculations and measurements for both the return losses and the radiation patterns. The gain is around 6.5 dBi, and the radiation patterns have broad single beams with a front-to-back ratio around 8 dB. The proposed antennas should find application in multiband wireless communications and also as array elements in future systems.

ACKNOWLEDGMENTS

This work has been partially supported by funding from the Spanish Ministry of Education under project no. TIC2002-04255-C04-02 and FEDER funds under project no. UMHE03-23-028. The authors want to express their gratitude to Juan Pedro Espinosa Lidón for his assistance with the antennas construction.

REFERENCES

1. G. Kumar and K.P. Ray, Broadband microstrip antennas, Artech House, Boston, 2003.
2. E. Ávila-Navarro and C. Reig, Bow-tie antenna: Optimal point for coaxial feeding. Proc ICEAA'03, Torino, Italy, 2003.
3. E.A. Navarro, A. Luximon, I.J. Craddock, D.L. Paul, and M. Dean, Multilayer and conformal antennas using synthetic dielectric substrates, IEEE Trans Antennas Propagat 51 (2003), 905–908.

4. F. Tefiku and C.A. Grimes, Desing of broad-band and dual-band antennas comprised of series-fed printed-strip dipole pairs, IEEE Trans Antennas Propagat 48 (2000), 895–900.
5. H.K. Smith and P.E. Mayes, Log-periodic array of dual-feed microstrip patch antennas, IEEE Trans Antennas Propagat 39 (1991), 1659–1664.
6. P.S. Hall, Application of the log-periodic technique to microstrip series arrays, IEE Proc H 133 (1986), 127–136.
7. B.L. Ooi, K. Chef, and M.S. Leong, Log-periodic slot antenna array, Microwave Opt Technol Lett 25 (2000), 24–27.
8. G. Augustin, S.V. Shynu, C.K. Aanandan, P. Mohanan, and K. Vasudevan, A novel electronically scannable log-periodic leaky-wave antenna, Microwave Opt Technol Lett 45 (2005), 163–165.
9. C. Reig, E. Navarro, and V. Such, FDTD analysis of E-sectoral horn antennas for broadband applications, IEEE Trans Antennas Propagat 10 (1997), 1484–1487.
10. C.A. Balanis, Antenna theory analysis and design, Wiley, New York, 1997.
11. Y. Qian, W.R. Deal, N. Kaneda, and T. Itoh, A microstrip-fed quasi-Yagi antenna with broadband characteristics, Electron Lett 34 (1998), 2194–2196.

MICROSTRIP STEPPED-IMPEDANCE HAIRPIN RESONATOR LOW-PASS FILTER WITH DEFECTED GROUND STRUCTURE

Ju-Hyun Cho and Jong-Chul Lee
RFIC Research and Education Center
Kwangwoon University
447-1 Wolgye-dong, Nowon-ku
Seoul 139-701, Korea

Received 5 August 2005

ABSTRACT: *In this paper, a new microstrip stepped-impedance hairpin resonator (SIR) low-pass filter (LPF) using a defected ground structure (DGS) is proposed. The proposed SIR hairpin low-pass filter using DGS provides a very sharp cutoff frequency response with low insertion loss. Furthermore, the SIR hairpin low-pass filter can provide attenuation poles for the wide-stopband characteristic due to the resonance characteristic of the DGS. Design parameters for the SIR low-pass filter are derived based on stepped-impedance theory and the equivalent-circuit model for the DGS. The experimental results show excellent agreement with the theoretical simulation results.* © 2005 Wiley Periodicals, Inc. Microwave Opt Technol Lett 48: 405–408, 2006; Published online in Wiley InterScience (www.interscience.wiley.com). DOI 10.1002/mop.21364

Key words: *stepped impedance hairpin resonator (SIR); low-pass filter; aperture; defected ground structure (DGS)*

1. INTRODUCTION

The defected ground structure (DGS) is realized by etching a defected pattern on the ground plane. Initially, a microstrip line with a dumbbell-shaped pattern of DGS was presented and excellent bandgap effects in microwave frequencies were obtained [1]. Now, the DGS is being applied widely to the design of microwave and millimeter-wave circuits. DGS with uniform square-patterned defects for planar circuit, which provides excellent stopband and slow-wave characteristics, was reported and used in the design of oscillators and amplifiers [2, 3].

In this paper, a new etched DGS shape for the implementation of an SIR hairpin low-pass filter is proposed. An etched defected pattern disturbs the shield current distribution on the ground plane [4, 5]. This disturbance can change the characteristics of a transmission line, such as line capacitance and inductance [6, 7]. The proposed SIR hairpin low-pass filter using DGS consists of narrow and wide etched areas in the backside metallic ground plane, which give rise to an increase of the effective capacitance and inductance of a transmission line, respectively, as well as the resonant frequency of stepped-impedance hairpin resonators. Thus, an LC equivalent circuit can be modeled for the proposed DGS circuit unit.

Small-size low-pass filters are frequently required in many communication systems to suppress harmonics and spurious signals [8–11]. The conventional stepped-impedance and Kuroda-identity-stub low-pass filters only provide Butterworth and Chebyshev characteristics with a gradual cutoff frequency response. These types of filters require more sections to obtain high performance, which causes an increase in the size of the filter and insertion loss. A compact semilumped low-pass filter has been also proposed, but the structure using lumped elements increases the difficulties of fabrication [12].

The microstrip stepped-impedance resonator (SIR) low-pass filter using DGS exhibits advantages of high performance, low cost, and easy fabrication.

In this paper, an equivalent-circuit model for the stepped-impedance hairpin resonator and unit DGS are described. The dimensions of the filter are optimized via electromagnetic (EM) simulation. A microstrip stepped-impedance hairpin resonator low-pass filter using DGS is adopted in order to suppress the 2^{nd}-harmonic component, achieve a broad stopband bandwidth, and improve the skirt characteristic.

2. ANALYSIS OF THE STEPPED-IMPEDANCE HAIRPIN RESONATOR

Figure 1 shows the basic layout of the stepped-impedance hairpin resonator. The stepped-impedance hairpin resonator consists of the single transmission line l_s and coupled lines with a length of l_c. Z_h is the characteristic impedance of the single transmission line l_s. Z_{0e} and Z_{0o} are the even-mode and odd-mode impedances, respectively, of symmetric capacitance-loaded parallel coupled lines with a length of l_c. By selecting $Z_h > \sqrt{Z_{0e}Z_{0o}}$, the size of the stepped-impedance hairpin resonator becomes smaller than that of the conventional hairpin resonator, which is an elliptic-function low-pass filter using microstrip SIR hairpin resonator [13]. Also, interferences from higher-order harmonics can be reduced by employing the DGS on the ground plane.

The resonator structure to be considered here is shown in Figure 1(a). The SIR is symmetrical and has two different characteristic impedance lines, Z_h and Z_l (or admittances, Y_h and Y_l).

The admittance of the resonator from the open end, Y_i, is given by

$$Y_i = jY_1 \frac{2(K\tan\theta_1 + \tan\theta_2)\cdot(K - \tan\theta_1\cdot\tan\theta_2)}{K(1-\tan^2\theta_1)\cdot(1-\tan^2\theta_2) - 2(1+K^2)\cdot\tan\theta_1\cdot\tan\theta_2}, \quad (1)$$

where K is the impedance ratio ($=Z_l/Z_h$). The resonance condition can be obtained from the following equation:

$$Y_i = 0. \quad (2)$$

From Eqs. (1) and (2), the fundamental resonance condition can be expressed as